CHEMBIOCHEM

Imaging Target mRNA and siRNA-Mediated Gene Silencing In Vivo with Ribozyme-Based Reporters

Min-Kyung So ,[a, b] Gayatri Gowrishankar,[a] Sumitaka Hasegawa,[a] June-Key Chung,[b] and Jianghong Rao*[a]

Noninvasive imaging of specific mRNAs in living subjects promises numerous biological and medical applications. Common strategies use fluorescently or radioactively labelled antisense probes to detect target mRNAs through a hybridization mechanism, but have met with limited success in living animals. Here we present a novel molecular imaging approach based on the group I intron of Tetrahymena thermophila for imaging mRNA molecules in vivo. Engineered trans-splicing ribozyme reporters contain three domains, each of which is designed for targeting, splicing, and reporting. They can transduce the target mRNA into a reporter mRNA, leading to the production of reporter enzymes that can be noninvasively imaged in vivo. We have demonstrated this ribozyme-mediated RNA imaging method for imaging a mutant p53 mRNA both in single cells and noninvasively in living mice. After optimization, the ribozyme reporter increases contrast for the transiently expressed target by 180-fold, and by ten-fold for the stably expressed target. siRNA-mediated specific gene silencing of p53 expression has been successfully imaged in real time in vivo. This new ribozyme-based RNA reporter system should open up new avenues for in vivo RNA imaging and direct imaging of siRNA inhibition.

Introduction

Fluorescence in situ hybridization (FISH) has for many years been the mainstay for examining the expression and localization of various RNA species.[1] Recently, several new RNA imaging techniques have been developed and allow the visualization of single RNA transcripts in living cells. These techniques include the use of molecular beacons that fluoresce only when the probes hybridize to the target.[2] A number of efforts have also been made to use radiolabeled antisense oligonucleotides (RASONs),[3,4] which are generally modified nucleic acids (for example, phosphothioates, 2′-OMe backbone, peptide nucleic acids) and labeled with a radioisotope for imaging overexpressed RNA targets.

In spite of these advancements, it has proven difficult to use labeled oligo probes to image mRNA molecules in living animals; this is mainly due to issues related to the in vivo stability and specificity of the probes, as well as problems with their in vivo delivery to target tissue and a poor signal-to-noise ratio due to the inherently low copy number of mRNA. These drawbacks have necessitated the development of alternate techniques for in vivo RNA imaging. Bhaumik et al. developed a system based on the mammalian spliceosome to image pre-mRNA in vivo.[5] The technique, known as spliceosome-mediated RNA trans-splicing (SMaRT), was originally developed with the intention of repairing disease-causing mutant genes at the level of pre-mRNA.[6,7] Another approach for live imaging of a target mRNA uses a genetically encoded reporter based on an RNA binding protein and a fluorescent protein.[8] This dual- or three-component (if the fluorescent protein is split into two separate parts) reporting system has been demonstrated with a number of RNA targets containing genetically fused RNA aptamer tags in living cells,[9,10] and even with endogenous RNAs in mitochondria.[11] We used a different approach and exploited the enzymatic activity of the natural Tetrahymena group I intron to develop a novel RNA imaging tool, which employs antisense RNA binding and reporter gene systems to achieve targeting specificity and signal amplification, respectively.

The nuclear rRNA of the ciliated protozoan Tetrahymena thermophila contains a 413-nucleotide intervening sequence (IVS; also categorized as group I introns) that is excised from the larger RNA by self-splicing.[12] Deleting the first 21 nucleotides of the group I intron afforded a derivative known as L-21, which was shown to mediate trans-splicing (between two separate RNA molecules) in vitro,[13,14] in E. coli[15] and in mammalian cells.[16] The internal guiding sequence (IGS) of the ribozyme may be modified to base pair essentially with any sequence as long as a G–U wobble pair is maintained at the splice site. Because of this sequence latitude, ribozymes based on the

[a] M.-K. So ,+ Dr. G. Gowrishankar,+ Dr. S. Hasegawa, Prof. J. Rao
Molecular Imaging Program at Stanford
Department of Radiology, Biophysics, Cancer Biology Programs
Stanford University School of Medicine
1201 Welch Road, Stanford, California 94305-5484 (USA)
Fax: (+1) 650-736-7925
E-mail: jrao@stanford.edu

[b] M.-K. So ,+ Prof. J.-K. Chung
Department of Nuclear Medicine, Laboratory of Molecular Imaging and Therapy of Cancer Research Institute
Seoul National University College of Medicine
Yeongeon-dong, Jongno-gu, Seoul 110-744 (South Korea)

[+] These authors contributed equally to this work.

group I intron of *Tetrahymena* may be engineered to target any chosen RNA. Sequences present downstream of the ribozyme are ligated to the splice site of the substrate RNA. These 3′ exon sequences may also be changed to potentially any nucleotide sequence. This ability was thus used to "revise" various mutant RNA transcripts in a new gene therapy approach termed ribozyme-mediated RNA repair.

Compared with more traditional strategies, RNA repair would allow the endogenous regulation of the gene modification (as it is RNA-directed) and simultaneously reduce the expression of the mutant gene product. This approach has been successfully used to correct sickle cell transcripts,[17] to remedy the triplet repeat expansion in the 3′ UTR of the myotonic dystrophy protein kinase transcript,[18] to repair mutant p53 transcripts,[19] to repair the mutant mRNA of canine skeletal muscle chloride channel,[20] and to convert pathogenic transcripts of the hepatitis C virus (HCV) into new RNAs that exert anti-HCV activity.[21] These ribozymes have also been used to trans-splice a cytotoxic gene onto a particular target RNA,[22,23] ensuring target-specific expression of the cytotoxic gene. Whereas cleaving ribozymes must efficiently deplete a chosen mRNA species to be effective in vivo, even a small amount of trans-splicing would be sufficient to express the cytotoxic gene and kill the target gene-expressing cells.

In a novel application of the trans-splicing ribozymes, we attached reporter genes as the 3′ exon to detect the target RNA molecule in vivo. Guided by an attached antisense sequence, the designed ribozyme would splice the reporter onto the target RNA in-frame, resulting in a fusion RNA consisting of the reporter and part of the target. The fusion RNA can subsequently be translated to give the reporter activity. In this paper we demonstrate that this new RNA imaging tool is able to detect tumor-specific mutant p53 mRNA in living mice in real time. We further applied this ribozyme-based RNA reporter to image siRNA-mediated gene silencing in vivo.

Results and Discussion

Ribozyme reporter design

Trans-splicing ribozymes bind their RNA substrates through base-pairing to a 6 nt internal guide sequence (IGS) on the ribozymes. This is followed by two consecutive transesterification reactions that lead to the cleavage of the target mRNA and formation of a ligation product that contains the 5′ fragment of the target mRNA and the exon attached to the 3′ end of the ribozyme.[15,24,25] Based on the ribozyme-mediated trans-splicing mechanism, we designed trans-splicing ribozyme-based reporters to image a target mRNA (Figure 1).

The reporter construct consists of three domains: the trans-splicing ribozyme intron, the antisense sequence for target binding, and a reporting domain containing a reporter-gene mRNA. The start codon (AUG) of the reporter gene is removed to minimize the reporter translation before the trans-splicing. Trans-splicing between the ribozyme reporter and the mRNA target generates a fusion reporter gene that contains the start codon from the target mRNA and becomes translatable. The
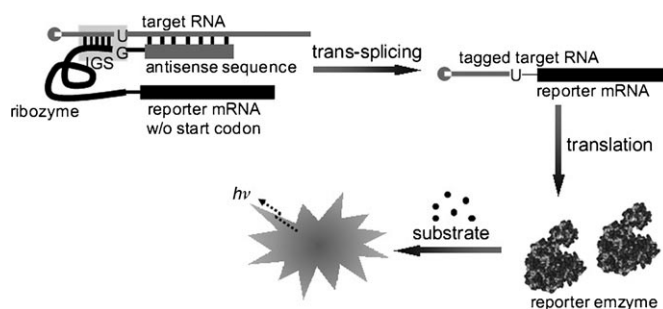

Figure 1. A schematic representation outlining the design of a ribozyme-based reporter for RNA detection.

translation product of the fusion reporter mRNA—the fusion enzyme reporter—catalyzes biochemical reactions and produces readout signals for in vivo imaging (Figure 1).

We constructed our first ribozyme reporter, TRz–β-lactamase (TRz–Bla), for imaging a dominantly negative mutant p53 (p53DN) mRNA (G-to-A mutation at nt 1017; Figure 2A). The p53 tumor suppressor gene is one of the most commonly mutated genes in human cancers, encoding a transcription factor that mediates cell-cycle arrest and apoptosis in response to DNA damage and cellular stresses.[26,27] The dominantly negative p53DN is functionally inactive even when overexpressed, and was thus used as our model target. A uridine located at position +41 (+ indicates the number of bases from the A of the start codon) on the p53 mRNA was previously identified to be accessible to the trans-splicing ribozyme as a splice site.[19] Therefore, TRz–Bla was directed at U41 on the p53DN mRNA with a 202 nt antisense sequence complementary to a region downstream of the U41 on the p53DN mRNA (from nt 49 to 250). The selection of this long targeting sequence is based on our previous finding that a longer antisense sequence leads to more efficient in vivo trans-splicing.[28] To further enhance trans-splicing potential, TRz–Bla has an extended IGS (9 nt) and a 7 nt P10 helix (Figure 2A). The coding sequence of a Bla reporter gene is attached to the 3′-end of the ribozyme through a 15-nt linker; this ensures that Bla will be spliced in frame to the p53DN mRNA at the splice site. While this reporter is designed for p53DN, it should image wild-type p53 as well if p53 mRNA is present at the detectable abundance, as both the splicing site (nt 41) and the targeting sequence (nt 49 to 250) are far away from the mutation site (nt 1017) in p53DN.

Imaging p53DN mRNA expression using ribozyme β-lactamase reporter

COS7 cells were chosen for this study because they have low endogenous p53 activity, and this would allow for the evaluation of targeting specificity. COS7 cells were cotransfected with TRz–Bla along with a plasmid expressing p53DN mRNA (pCMV–p53DN). The splicing reaction was assayed both at the RNA level by reverse-transcriptase PCR (RT-PCR) to detect the trans-splicing product and at the protein level to measure the reporter-enzyme Bla activity with a fluorometric assay (Figures 2B and C).[29] A time course analysis was performed to
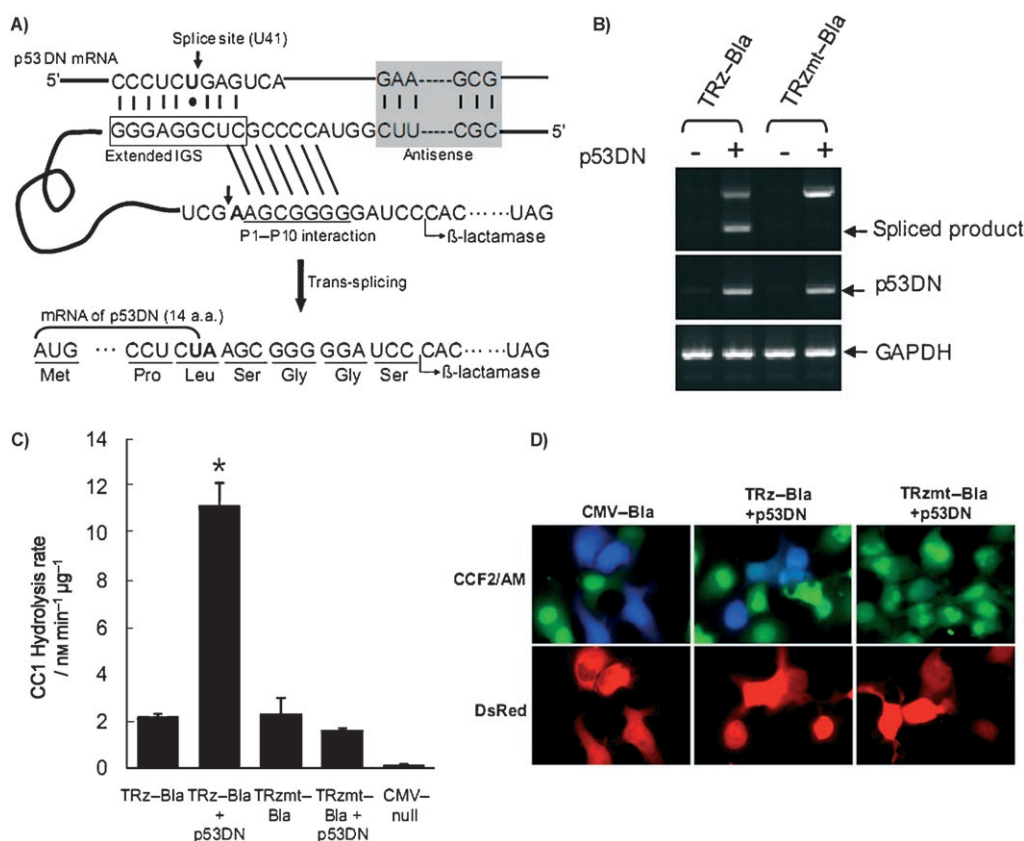
Figure 2. Ribozyme-mediated imaging of the p53DN mRNA with the ribozyme β-lactamase reporter (TRz–Bla). A) Schematic diagram of the ribozyme reporter (TRz–Bla) targeting the p53DN mRNA. Arrows indicate the 5′ splice site (U41) on the p53DN mRNA and the 3′ splice site on the ribozyme reporter. The shaded area downstream of the 5′ splice site marks the 202 nt antisense. The nine boxed nucleotides are extended IGS. The G–U wobble base-pair at the 5′splice site is indicated by a black dot (·). Oblique lines indicate the 7 bp P1–P10 interaction. B) RT-PCR analysis of RNA extracts from COS7 cells transfected with the indicated constructs. C) β-Lactamase activity in COS7 cells 72 h after transient transfection with indicated constructs, shown as the hydrolysis rate of CC1. An asterisk (*) denotes statistical significance ($p < 0.05$). D) Fluorescence microscopy images of COS7 cells transfected with indicated constructs and stained with CCF2/AM at 72 h after transfection. Upper panel shows an overlay of frames captured at 530 nm (green emission) and 460 nm (blue emission), and lower panel shows the DsRed positive cells (emission at 605 nm).

examine the kinetics of the splicing-dependant reporter activity, indicating the peak activity at 72 h after transfection (data not shown). RT-PCR and sequence analysis of these samples at the 72 h time-point confirmed that correct trans-splicing had occurred in cells expressing the target p53DN mRNA (Figure 2B). In comparison, when the control construct TRz$_{mt}$–Bla, an inactive mutant containing a single mutation at the catalytic site of the ribozyme (G264A),[28,30] was transfected along with pCMV–p53DN, no splice product was detected under the same conditions by RT-PCR (Figure 2B). The Bla reporter activity of cells cotransfected with TRz–Bla and pCMV–p53DN was seven-fold higher than that of cells cotransfected with the inactive reporter construct and pCMV–p53DN (Figure 2C). Other controls with only TRz–Bla or TRz$_{mt}$–Bla similarly displayed low Bla reporter activity (Figure 2C). These results demonstrate that the ribozyme reporter system can detect the specific target mRNA from a pool of cellular RNAs in transfected culture cells.

We then tested if we could visualize the detection of p53DN mRNA in living cells using a membrane-permeable fluorogenic substrate for β-lactamase, CCF2/AM.[31] COS7 cells were transfected with TRz–Bla or TRz$_{mt}$–Bla along with pCMV–p53DN. A mammalian expression vector expressing red fluorescent protein DsRed was cotransfected in all cases as a transfection marker. CCF2 fluoresces green (520 nm) because of fluorescence resonance energy transfer (FRET) from the coumarin donor to the fluorescein acceptor, but Bla hydrolysis splits off fluorescein, disrupts FRET, and shifts the emission to blue (447 nm).[32] Therefore, cells in general stained green but transfected cells exhibiting Bla activity (and in this case expressing p53 mRNA) emitted blue fluorescence from the cleaved substrate (Figure 2D). Quantitation of the blue-green signals from the images with image analysis software revealed that 54% of cells transfected with the ribozyme reporter TRz–Bla and the target p53DN were Bla-positive (blue/green ratio > 1) in contrast to the negative control, (TRz$_{mt}$–Bla+p53DN) in which just 8% of transfected cells were Bla-positive (see Figure S1 in the Supporting Information). Similar heterogeneity of the activity among the transfected cell population has been observed with cis-splicing ribozyme[32] and may be related to the stochastic mRNA synthesis in mammalian cells. This result correlates well with the in vitro data and has demonstrated the feasibility of

imaging target mRNA in single living cells with the ribozyme-based imaging method.

Detecting transiently expressed p53 mRNA in vitro with ribozyme-luciferase reporter

Our next quest was to apply the ribozyme reporter construct to image the p53DN mRNA in living animals. Firefly luciferase (FL) is an excellent reporter for bioluminescence imaging in small living animals.[33–35] We thus replaced the β-lactamase reporter with the firefly luciferase gene and constructed our second ribozyme reporter, TRz–FL (Figure 3A). RT-PCR and luciferase activity assays were completed to evaluate TRz–FL, and confirmed that TRz–FL could detect transfected p53DN in vitro. Similar to TRz–Bla, the splicing-dependant activity peaked at about 72 h (Figure 3B). Northern blot analysis was performed to assay the specificity of the trans-splicing reaction. COS7 cells were transfected with TRz–FL or TRz$_{mt}$–FL (an inactive mutant with the same mutation in the ribozyme as TRz$_{mt}$–Bla) along with or without p53DN. While the unspliced reporter RNA was detected in all four samples, the splice product generated by the trans-splicing was observed only in cells transfected with both TRz–FL and the target p53DN (Figure 3C). Moreover, no major nonspecific splice products were detected in the blot; this suggests that the trans-splicing reaction proceeded between the ribozyme reporter TRz–FL and the target p53DN mRNA with a fair degree of specificity.

To examine the correlation between the splicing-dependant luciferase activity and the p53DN mRNA level, we varied the amounts of the p53DN plasmid during the cotransfection of COS7 cells with TRz–FL or TRz$_{mt}$–FL. The detection of the splice product by the RT-PCR analysis was dependent on the amount of target p53DN plasmid (Figure 4A). Quantitative RT-PCR revealed that both the p53DN mRNA from the trans-splicing reaction and the fusion mRNA increased linearly with the amount of plasmid transfected (Figures 4B and C). Correspondingly, the splicing-dependant luciferase activity also increased as the amount of plasmid transfected increased (Figure 4B). These results indicate a linear correlation between the measured splicing-dependent reporter activity and the target mRNA level and have demonstrated the feasibility of detecting the target mRNA quantitatively with the ribozyme-based reporter system.

Visualizing p53 mRNA expression in living animals

We next evaluated the efficacy of our constructs for imaging p53DN mRNA in living animals. As the first model, 2.5×10^6 COS7 cells transfected with either TRz–FL or TRz$_{mt}$–FL along with pCMV–p53DN or empty vector (pCMV–null), were subcutaneously implanted at four different positions on the bodies of nude mice ($n = 3$). Mice were imaged with a CCD camera immediately after i.p. injection of D-luciferin and every 24 h thereafter. The kinetics of the in vivo trans-splicing reaction in the mice followed a similar trend as observed in cell culture. Regions of interest (ROI) analysis revealed a maximum of ninefold difference between the tumor expressing both the target p53DN and the ribozyme reporter TRz–FL and the background bioluminescence from the other three control tumors 72 h after transfection (Figures 5A and 5B). RT-PCR analysis of RNA extracted from the tumors and sequencing of the PCR product revealed that correct trans-splicing had occurred (Figure 5C).

The second model employed the hydrodynamic delivery of TRz–FL and p53DN to the liver of a nude mouse, and examined the trans-splicing in transfected liver cells by in vivo bioluminescence imaging. The hydrodynamic method of delivery uses a large injection volume and short injection time, resulting in an accumulation and subsequent expression of plasmid DNA, predominantly in the liver.[36–38] Mice were imaged at an interval of 6 or 12 h after the plasmid injection (Figure 6A). ROI analysis revealed that at 24 h the total bioluminescent emission from the mice injected with both TRz–FL and pCMV–p53DN was seven-fold stronger than from the mice injected only with TRz–FL (Figure 6B). The contrast between the two groups increased up to 28-fold at 36 h. Ex vivo imaging of ex-
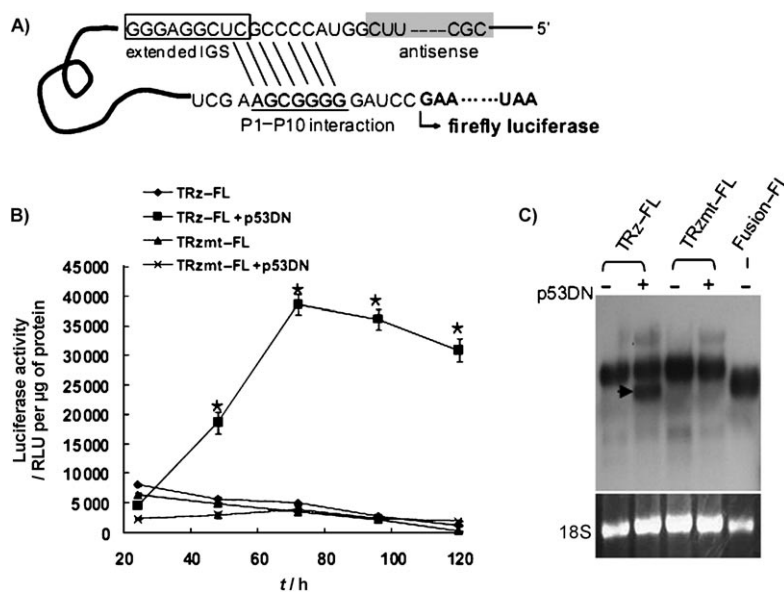

Figure 3. Detection of the p53DN mRNA with the ribozyme firefly luciferase reporter (TRz–FL). A) Schematic diagram of TRz–FL targeting the p53DN mRNA. B) Splicing-dependant luciferase activity in COS7 cells transfected with the indicated constructs (RLU per μg protein) versus time (h). An asterisk (*) denotes statistical significance ($p < 0.05$). C) Northern blotting assay of cells transfected with indicated constructs with DIG-labeled luciferase DNA probe. The spliced reporter mRNA is indicated by an arrow. The spliced mRNA is similar in size to the p53 luciferase fusion RNA (fusion-FL) expressed from a CMV promoter (right lane). Ethidium bromide staining of the 18S rRNA before transfer is shown below.
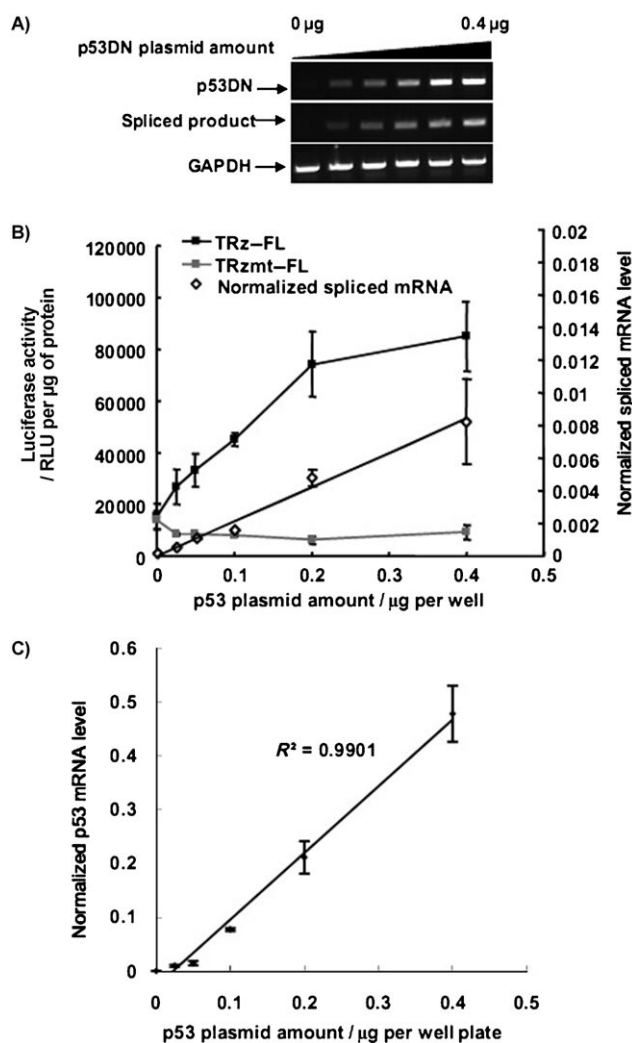
Figure 4. Quantitative correlation of splicing-dependant luciferase activity to p53DN mRNA level. A) RT-PCR analysis of COS7 cells transfected with increasing amounts of the p53DN plasmid. B) Dependence of the p53DN mRNA level and the reporter activity on the amount of p53DN plasmid used in transfection. The amount of TRz–FL or TRz$_{mt}$–FL is constant in all transfections. Fusion reporter mRNA levels are measured by quantitative PCR and normalized to GAPDH RNA, showing a good correlation of $R^2 = 0.99$. C) There is a linear relationship between the amount of p53DN plasmid and its mRNA level.

cised organs from both mice 24 h after the plasmid injection corroborated this result (See Figure S2 in the Supporting Information). RT-PCR analysis of RNA extracts from livers confirmed the correct trans-splicing at the RNA level (Figure 6C). The small amount of the splice product detected in the negative controls could be due to trans-splicing to endogenous p53 mRNA in the mouse liver as shown in Figure 6C; we mentioned previously that the reporter was able to target and image wild type p53 as well.

Improving the sensitivity of the reporter for imaging stably expressed p53DN mRNA

The ribozyme firefly-luciferase reporter TRz–FL is able to detect overexpressed p53DN mRNA in vivo, but its sensitivity does not allow the detection of stably expressed p53DN mRNA in vivo. One approach to improving the sensitivity is to minimize the nonsplicing-related background signal such as leaky translation of the reporter gene before trans-splicing. We decided to further truncate the firefly luciferase gene and delete three additional amino acids after the first methionine. Moreover, the nucleotides that code for the amino acids in position 5–7 of the luciferase are involved in the formation of a 9 bp helix (P1–P10 interaction) with the 5′ end of the ribozyme (Figure 7A); this helix is believed to be important for positioning the 3′ exon (luciferase gene) for trans-splicing and blocking leaky translation from the luciferase before splicing. This new reporter TRz–FL2 indeed showed much lower background activity than TRz–FL.

We tested TRz–FL2 similarly with transiently or stably expressed p53DN gene in COS7 cells. The negative control was an inactive version of TRz–FL2 with a single mutation (TRz$_{mt}$–FL2). Trans-splicing was assayed at both the RNA level (Figure 7B) and the protein level by assessing luciferase activity (Figure 7C). A 180-fold contrast was observed in the transient transfection in which the pCMV–p53DN was present in excess; this is much larger than that with TRz–FL, which is about seven-fold. For the stable transfection of pCMV–p53DN, the contrast was readily detectable with a value of as high as ten-fold (Figure 7C inset), although the expression level of stably transfected p53DN is much lower than that in the transient transfection as measured by RT-PCR (Figure 7D). The ability to detect of stably expressed target mRNA using our improved TRz–FL2 reporter in vivo suggests that it should be feasible to detect an endogenous mRNA target that is expressed at the similar abundance.[39]

Imaging siRNA-mediated gene silencing in vivo

After having established that the ribozyme reporter could image the expression of specific mRNA in both living cells and living animals, we applied it to image RNAi-mediated suppression of target gene expression in vivo. Gene silencing by small interference RNAs offers a powerful yet convenient means to intervene in gene expression, and assessment of the silencing effect in vivo by direct visualization should facilitate many biological and medical applications. In previous studies siRNA-directed inhibition of expression was often assessed with a reporter gene such as green fluorescent protein or a fusion construct containing the target gene and the reporter gene as the target.[40–42]

Two p53-gene specific siRNAs (siRNA#1 targeted at nucleotides starting from the position 943 and siRNA#2 at the position 1030) and appropriate negative control siRNA were synthesized commercially. The siRNAs were cotransfected with TRz–FL2 and the p53DN construct in COS7 cells. As shown in Figure 8A, the p53-splicing-dependant luciferase signal dropped significantly by more than nine-fold in the presence of the p53-specific siRNA but not with the negative-control siRNA. More importantly, the drop in the luciferase activity was consistent with the decrease in the p53 RNA levels determined by quantitative RT-PCR (Figure 8A).
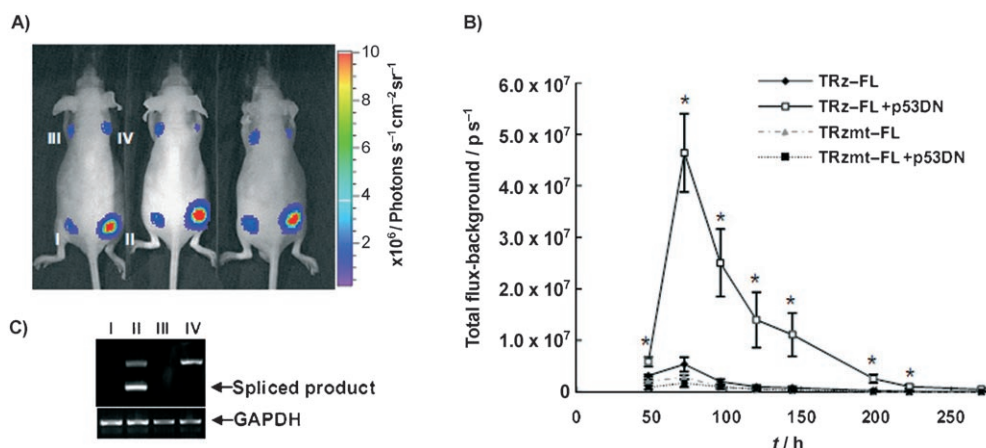
Figure 5. Bioluminescence imaging of the p53DN mRNA in implanted cells in living mice. A) Representative images of nude mice with subcutaneous implantation of COS7 cells that were transiently transfected with TRz–FL+pCMV-null (I), TRz–FL+ pCMV-p53DN (II), TRz$_{mt}$–FL+pCMV-null (III), or TRz$_{mt}$–FL+pCMV-p53DN (IV), at indicated positions. B) ROI analysis of bioluminescent signals emitted as a function of the time (h) after initial plasmid transfection. C) RT-PCR results from total RNA isolated from tumors 24 h after implantation.
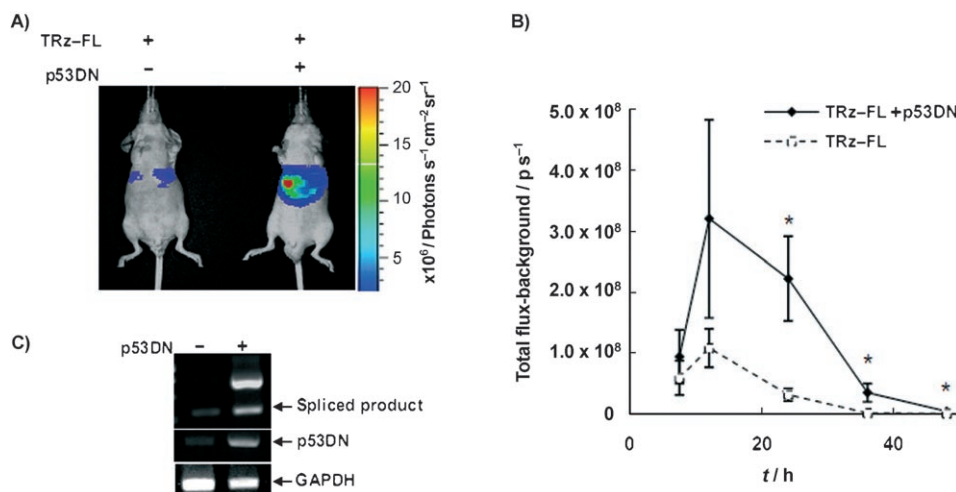

Figure 6. Bioluminescence imaging of systemically delivered ribozyme firefly-luciferase reporter in living mice. A) Representative bioluminescent imaging of mice 24 h after intravenous injection of the ribozyme luciferase reporter (TRz–FL) and the pCMV–p53DN (right) or an empty vector (left). B) ROI analysis of bioluminescence from mice imaged at different times after the plasmid injections. C) RT-PCR results of total RNAs from liver dissects of mice 24 h after the injection. An asterisk (*) denotes statistical significance ($p < 0.05$).

We next examined the correlation between the amount of p53-specific siRNA and the reporter signal. Varying concentrations of siRNA#1 were added to COS7 cells in cotransfection with the ribozyme and p53DN constructs. The luminescent output from the cells was captured using cooled CCD cameras 72 h after transfection (Figure 8B), and the p53 mRNA level in the respective samples was measured by quantitative RT-PCR. Quantification of the signals by the ROI method revealed a significant correlation ($R^2 = 0.97$) between the splicing-dependant luminescent signal and the p53 mRNA level (Figures 8C and Figure S3 in the Supporting Information). A silencing effect of as low as 16 pM of siRNA was readily detectable with the ribozyme reporter. These results suggest that the ribozyme reporter system allows quantitative estimates of the efficacy of siRNA suppression.

We finally evaluated the utility of our ribozyme reporter system in imaging the siRNA efficacy in preclinical animal models. The TRz–FL2 and the p53DN expressing constructs were delivered through hydrodynamic injections to the livers of nude mice ($n = 6$–8 each group), along with p53-specific siRNA#1 or negative control siRNA. An 87% drop in the splicing-dependant luciferase signal was observed only in the mice injected with the p53 siRNA#1 (Figures 8D and E). The RT-PCR results with the RNA extract from the livers of a sample set of these mice confirmed that the drop in the luciferase output correlated to the p53 RNA levels (See Figure S4 in the Supporting Information). Our data demonstrate that the ribozyme reporter is able to image the siRNA suppression of target gene expression in vivo.

Conclusions

We have reported a trans-splicing ribozyme-based reporter system to image target mRNAs in living subjects, and successfully imaged a mutant p53 mRNA in single cells and living mice. Different from existing methods for mRNA imaging, this new approach offers several attractive features: The two-step amplification promises great sensitivity for the target detection. The method is compatible with many in vivo noninvasive imaging modalities, for example, positron emission tomography (PET) or magnetic resonance imaging (MRI), if a PET or MRI
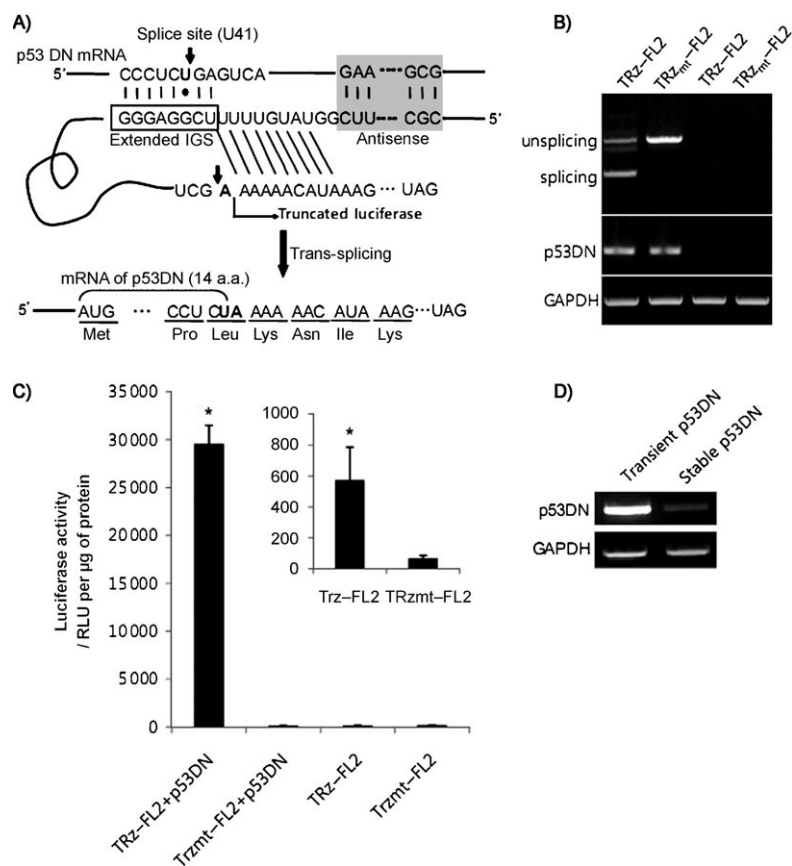
enormous applications in both biological and biomedical research from evaluating the in vivo specificity and efficacy of siRNAs to in vivo screening siRNA for therapeutics.

Figure 7. Improved ribozyme luciferase reporter TRz–FL2. A) Schematic diagram of TRz–FL2 targeting the p53DN mRNA. Arrows indicate the 5′ splice site (U41) on the p53DN mRNA and the 3′ splice site on the ribozyme reporter. Shaded area downstream of the 5′ splice site marks the 202 nt antisense sequence. Boxed eight nucleotides are extended IGS. The G–U wobble base-pair at the 5′splice site is indicated by a black dot (·). Oblique lines indicate the 9 bp P1–P10 interaction. The p53-luciferase fusion mRNA generated by trans-splicing is also shown. B) RT-PCR of RNA from COS7 cells transfected with indicated ribozyme constructs; the first two lanes from left contained p53DN and the last two lanes did not. C) Luciferase activity in COS7 cells transiently or stably (inset) transfected with the indicated constructs. D) RT-PCR analysis of p53DN RNA levels in transiently or stably transfected COS7 cell lines.

reporter gene other than Bla or luciferase is attached. The reporter constructs can be easily delivered into any cell line or in vivo into mice through plasmid- or viral-based vectors.

While this study uses a mutant p53 as the target, any new mRNA target can first be mapped for splice sites with an RNA library, and corresponding antisense sequences can then be added in the reporter for targeting.[17] Our optimized reporter has shown the feasibility of applying this strategy to direct imaging of an endogenous mRNA, especially overexpressed tumor-specific mRNA in living subjects.

Although we have shown that this method can visualize target mRNA in single living cells with Bla as the reporter enzyme, it may not offer subcellular resolution due to the signal amplification scheme that leads to the separation of the RNA location from the final readout signals. The need of a substrate for signal generation may also exclude it from visualizing fast RNA dynamics.

The utility of this reporter has been further demonstrated in direct imaging of the siRNA-mediated specific suppression in gene expression. Imaging siRNA inhibition in vivo should find

Experimental Section

All experiments performed on mice were approved by the Stanford Institutional Animal Care and Use Committee.

Plasmid construction: All mammalian expression vectors were constructed by standard cloning procedures. PCR amplification was done using Pfu ultra-high-fidelity DNA polymerase from Stratagene (La Jolla, CA, USA) to avoid the introduction of any undesirable mutations. The ribozyme sequence was derived from pTT1A3-T7 (a kind gift from Drs. Thomas Cech at University of Colorado and Roger Tsien at University of California, San Diego). The gene encoding β-lactamase without the secretory signal and the start codon was derived from pUC19 (New England Biolabs, Ipswich, MA, USA). The gene encoding firefly luciferase without the start codon was derived from pGL3 (Promega, Madison, WI, USA). The p53 antisense sequence was derived from pCMV–p53wt (Clontech, Mountain View, CA, USA). The pDsRed2-N1 vector (Clontech) was used as the plasmid backbone in constructing a CMV promoter-driven expression vector after removal of the DsRed cDNA (pCMV–null). pCMV–p53DN (Clontech) expresses a dominant negative mutant of the tumor suppressor gene p53.

Cell lines, cell culture, and transfection protocols: COS7 cells (monkey kidney cell line) were grown in Dulbecco's Modified Eagle medium supplemented with 10% fetal bovine serum at 37 °C and 5% CO_2. Cells were transfected with Lipofectamine 2000 (Invitrogen Corp., Carlsbad, CA, USA) according to the manufacturer's protocol. Lysates for β-lactamase or luciferase activity assays were made using Passive Lysis Buffer (Promega).

RNA extraction and RT-PCR: Total RNA was isolated using TRIzol reagent (Invitrogen), and tissue samples were homogenized with Power Gen 125 (Fisher Scientific, Santa Clara, CA, USA) before RNA extraction. Isolated RNAs were treated with DNase before cDNA synthesis with M-MLV reverse transcriptase (Invitrogen). L-argininamide (50 mM) was present in both DNase treatment and cDNA synthesis to quench any in vitro trans-splicing. The cDNAs were amplified for 26 cycles unless otherwise specified using GoTaq (Promega). Quantitative RT-PCR was done with Brilliant SYBR Green QPCR mix from Stratagene and the iCycler from Bio-Rad (Hercules,
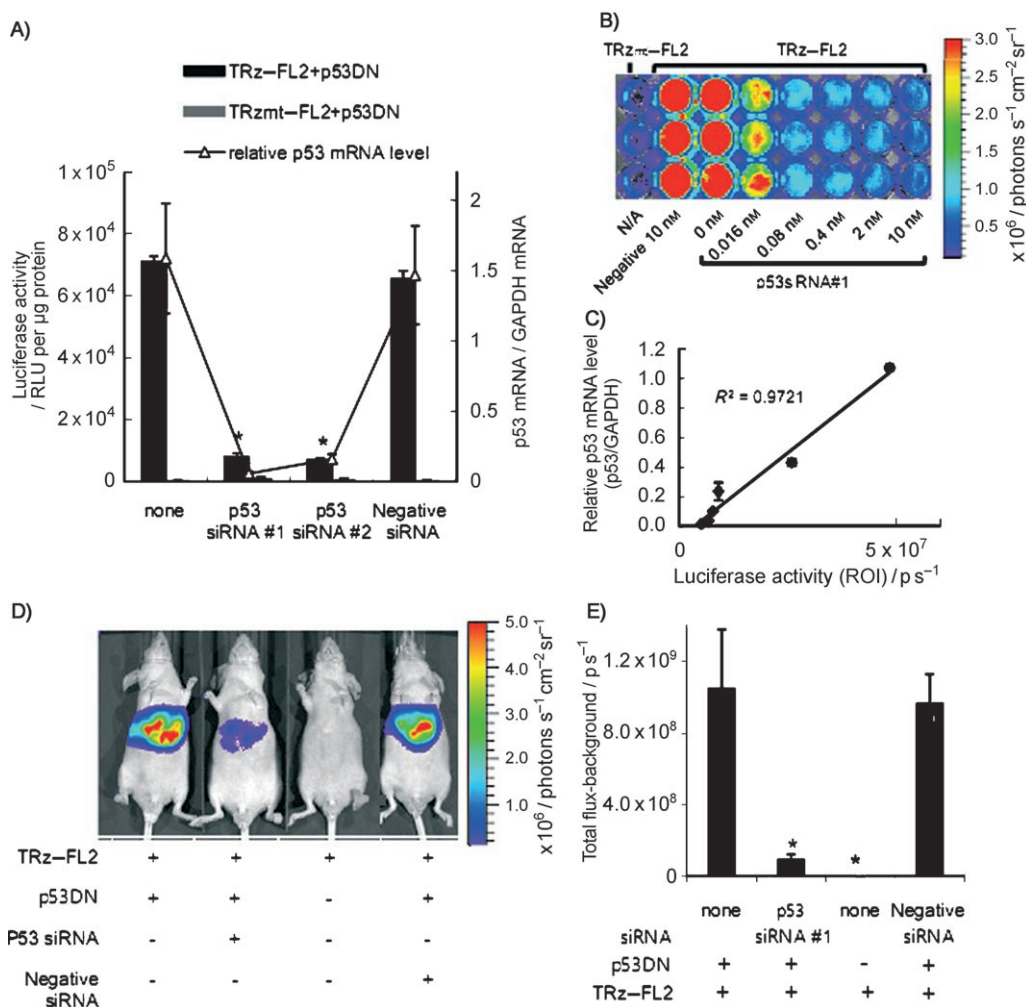
Figure 8. Imaging siRNA-mediated suppression of p53DN expression in vivo. A) Plot showing luciferase activity and p53DN mRNA levels of COS7 cells transfected with the indicated constructs and p53-specific siRNA or negative-control siRNA. mRNA levels were calculated by quantitative RT-PCR. B) Bioluminescent image of live COS7 cells transfected with TRz–FL2 or TRz$_{mt}$–FL2 and the indicated concentrations of negative siRNA or p53 siRNA#1. C) Plot showing p53 mRNA levels calculated by quantitative RT-PCR as a function of luciferase activity calculated by drawing ROIs in the image shown in Figure 7 B. D) Representative bioluminescent imaging of mice 24 h after hydrodynamic delivery of TRz–FL2, pCMV–null and pCMV–p53DN with negative siRNA, or p53 specific siRNA as indicated. E) ROI analysis of bioluminescence from mice imaged 24 h after plasmid and siRNA delivery. Asterisk (*) denotes statistical significance ($p < 0.05$).

CA, USA). Primers used were: splicing FW (TCG AGC CCC CTC TAA GCG), Luc BW (GCC CAA CAC CGG CAT AAA G) for the fusion product; p53FW (CAG TCA GAT CCT AGC GTC G) and Luc BW for detecting both unspliced and spliced products. PCR products were analyzed by gel electrophoresis in 1% agarose gels. The identities of the spliced products were revealed by sequence analysis. Quantitative RT-PCR was analyzed with an algorithm, Miner, developed by Zhao et al.[43]

Northern blotting: Total RNA (10 μg, or 5 μg for the control) was separated by denaturing 1% agarose gels in MOPS (20 mм, pH 7.0), EDTA (1 mм), sodium acetate (5 mм), and formaldehyde (6.8%). RNA was blotted onto nylon membranes (Hybond-N$^+$, Amersham, Piscataway, NJ, USA) by capillary transfer. Specific RNAs were detected by hybridization to DIG-labeled DNA probes (700 bp in size) against the firefly luciferase mRNA according to the manufacture's instructions (Roche Applied Sciences).

In vitro enzyme assays: To measure β-lactamase activity, cell lysate (45 μL) and fluorogenic substrate CC1 (1 mм, 5 μL)[29] were mixed in each well of a 96-well microtiter plate (Corning, Corning,

NY, USA). Fluorescence was measured with excitation at 360 nm and emission at 465 nm at each time point in a Safire microplate reader (TECAN, Research Triangle Park, NC). Fluorescence data was normalized against total lysate protein contents determined by a Bradford assay (Bio-Rad, Hercules, CA, USA). Bioluminescence assays were performed by using a TD 20/20 luminometer (Turner designs, Sunnyvale, CA). Cell lysates (20 μL) were mixed with LARII (Promega, Madison, WI, USA), and the reaction was measured in relative light units (RLU) in the luminometer. The values were normalized against protein content and reported as RLU per μg protein.

Fluorescence microscopy imaging: COS7 cells were transfected with the respective plasmids (0.4 μg each) along with pDsRed2-N1 (0.2 μg) by lipofectamine 2000 in a 24-well plate. 24 h after transfection, cells were reseeded onto a 35 mm glass bottom culture dish (MatTek, Ashland, MA). 48 h after reseeding, cells were washed twice with Hanks' balanced salt solution (HBSS, Sigma, St. Louis, MO, USA) and loaded for 1 h at room temperature with HBSS containing CCF2/AM (2 μм, Invitrogen), and probenecid (2.5 mм, Sigma). Cells were then washed four times with HBSS and ob-

served immediately under an Axiovert 200M fluorescence microscope (Carl Zeiss MicroImaging, Inc., Thornwood, NY, USA). The following filter set (Chroma Technology Corp., Rockingham, VT, USA) was used for microscopic analysis of CCF2/AM: HQ405/20 for excitation, 425DCXR as the dichroic mirror, HQ460/40 for blue emission, and HQ530/30 for green emission. For the acquisition of DsRed images the following filter set was used (Chroma): excitation, HQ546/12; dichroic mirror, Q560LP; emission, HQ605/75. Images were analyzed with METAMORPH software (Universal Imaging, Downingtown, PA). Quantitative analysis was done by using the MetaMorph Image analysis software version 5.0 (Universal Imaging, Downingtown, PA). Suitable thresholds were set in the images to be analyzed to enable selection of region of interests (ROIs). ROIs were then drawn around DsRed positive (transfected) cells and blue and green intensities were measured for each ROI after subtraction from background.

Cell implantation: 48 h after transfection, COS7 cells were collected by trypsinization, counted and suspended in phosphate buffered saline (PBS). Nude mice (four weeks old from Charles River Breeding Laboratories, Wilmington, MA), were anesthetized with isofluorane in the light-tight chamber of an IVIS 50 imager (Xenogen, Alameda, CA). After anesthetization, cells transiently transfected with the respective constructs (2.5×10^6 cells in 50 μL of PBS+50 μL of matrigel) were implanted s.c on the left and right shoulders and thighs.

siRNA sequences: siRNA duplexes against p53 (p53 siRNA#1, #2 are from Invitrogen, Validated stealthTM RNAi DuoPak): p53 siRNA#1 targets at the position 943: 5′-CCA UCC ACU ACA ACU ACA UGU GUA A-3′; p53 siRNA#2 targets at the position 1030: 5′-CCA GUG GUA AUC UAC UGG GAC GGA A-3′; in vitro nontargeting control duplex (negative siRNA, Ambion, Silencer Negative Control #1 siRNA); in vivo nontargeting control duplex (negative siRNA, Invitrogen, Stealth RNAi Negative Control 36% GC Content). p53 siRNA #1 and negative siRNA for in vivo experiments were purified through desalting.

In vitro siRNA and plasmid transfection: COS7 cells were seeded at a density of 5×10^4 cells per well in a 24-well plate, and transfected at 80% confluency with Lipofectamine 2000 (Invitrogen) following the manufacturer's instructions. Cells were cotransfected (in triplicate) with a mixture of expression plasmid (400 ng), target plasmid (400 ng) and siRNA (final concentration 10 nm per transfection), diluted to 50 μL in optiMEM medium (Invitrogen). Lipofectamine 2000 (2 μL) was diluted in optiMEM medium (50 μL) and incubated at room temperature for 5 min. This mixture was added to the nucleic acid and incubated for 20 min at room temperature, before addition to the plated cells. 72 h after transfection, bioluminescence assays, RT-PCR or quantitative RT-PCR were performed.

For cell plate images with different concentration of siRNA, COS7 cells were seeded in a 48-well plate and all materials were used in 1/3 of the 24-well-plate transfection method. Final concentration of siRNA was between 0.016 and 10 nm. 72 h after transfection, D-luciferin (3 mg in 100 μL PBS) was added to each well and incubated at room temperature for 5 min. The entire plate was imaged for 10 s using the IVIS in vivo imaging system.

In vivo delivery of plasmids and siRNA to mice: The use of hydrodynamic injections for plasmid delivery to the liver of mice has been described previously.[36] Briefly, plasmids were preincubated with 80 units of RNAse inhibitor (Invitrogen) at 37 °C for 30 min before use. All male nude (nu/nu) mice were ~28 g in weight (6–8 weeks of age) at the time of injection. Ribozyme plasmid DNA (50 μg) and target or pCMV–null plasmid DNA (50 μg) with siRNA (50 μg) was formulated in 5% w/v glucose in water (2 mL) and injected into the tail-vein of nude mice in one shot (injection time ~5 s, 26.5-gauge needle; Becton Dickinson and Company, Franklin lakes, NJ). Mice were imaged every 6 or 12 h thereafter.

Image acquisition and analysis: For small-animal bioluminescence imaging, a Xenogen in vivo Imaging System (IVIS; Xenogen) was used. Immediately before scanning, animals were anesthetized with isoflurane as before, and then injected via i.p with D-luciferin (3 mg per mouse). 10 min after D-luciferin injection, whole-body images were acquired for 5 or 1 min as per requirement. Regions of interest (ROIs) of constant area were manually drawn over areas of signal intensity by using the LIVING IMAGE software (Xenogen), and results were reported as maximum intensity values within an ROI in photons per second per cm^2 per steradian. A one-tailed student t test was used to calculate p values.

[1] A. M. Femino, F. S. Fay, K. Fogarty, R. H. Singer, *Science* **1998**, *280*, 585–590.
[2] D. P. Bratu, B. J. Cha, M. M. Mhlanga, F. R. Kramer, S. Tyagi, *Proc. Natl. Acad. Sci. USA* **2003**, *100*, 13308–13313.
[3] M. Touboul, A. S. Gauchez, M. D'Hardemare Adu, J. Lunardi, J. R. Deverre, C. Pernin, J. P. Mathieu, J. P. Vuillez, D. Fagret, *Anticancer Res.* **2002**, *22*, 3349–3356.
[4] M. K. Dewanjee, N. Haider, J. Narula, *J. Nucl. Cardiol.* **1999**, *6*, 345–356.
[5] S. Bhaumik, Z. Walls, M. Puttaraju, L. G. Mitchell, S. S. Gambhir, *Proc. Natl. Acad. Sci. USA* **2004**, *101*, 8693–8698.
[6] H. Chao, S. G. Mansfield, R. C. Bartel, S. Hiriyanna, L. G. Mitchell, M. A. Garcia-Blanco, C. E. Walsh, *Nat. Med.* **2003**, *9*, 1015–1019.
[7] X. Liu, Q. Jiang, S. G. Mansfield, M. Puttaraju, Y. Zhang, W. Zhou, J. A. Cohn, M. A. Garcia-Blanco, L. G. Mitchell, J. F. Engelhardt, *Nat. Biotechnol.* **2002**, *20*, 47–52.
[8] E. Bertrand, P. Chartrand, M. Schaefer, S. M. Shenoy, R. H. Singer, R. M. Long, *Mol. Cell* **1998**, *2*, 437–445.
[9] M. Valencia-Burton, R. M. McCullough, C. R. Cantor, N. E. Broude, *Nat. Methods* **2007**, *4*, 421–427.
[10] N. Daigle, J. Ellenberg, *Nat. Methods* **2007**, *4*, 633–636.
[11] T. Ozawa, Y. Natori, M. Sato, Y. Umezawa, *Nat. Methods* **2007**, *4*, 413–419.
[12] T. R. Cech, *Annu. Rev. Biochem.* **1990**, *59*, 543–568.
[13] T. Inoue, F. X. Sullivan, T. R. Cech, *Cell* **1985**, *43*, 431–437.
[14] M. D. Been, T. R. Cech, *Cell* **1987**, *50*, 951–961.
[15] B. A. Sullenger, T. R. Cech, *Nature* **1994**, *371*, 619–622.
[16] J. T. Jones, S. W. Lee, B. A. Sullenger, *Nat. Med.* **1996**, *2*, 643–648.
[17] N. Lan, R. P. Howrey, S. W. Lee, C. A. Smith, B. A. Sullenger, *Science* **1998**, *280*, 1593–1596.
[18] L. A. Phylactou, C. Darrah, M. J. Wood, *Nat. Genet.* **1998**, *18*, 378–381.
[19] T. Watanabe, B. A. Sullenger, *Proc. Natl. Acad. Sci. USA* **2000**, *97*, 8490–8494.
[20] C. S. Rogers, C. G. Vanoye, B. A. Sullenger, A. L. George Jr. , *J. Clin. Invest.* **2002**, *110*, 1783–1789.

[21] K. J. Ryu, J. H. Kim, S. W. Lee, *Mol. Ther.* **2003**, *7*, 386–395.

[22] B. G. Ayre, U. Kohler, H. M. Goodman, J. Haseloff, *Proc. Natl. Acad. Sci. USA* **1999**, *96*, 3507–3512.

[23] B. S. Kwon, H. S. Jung, M. S. Song, K. S. Cho, S. C. Kim, K. Kimm, J. S. Jeong, I. H. Kim, S. W. Lee, *Mol. Ther.* **2005**, *12*, 824–834.

[24] B. Sargueil, N. K. Tanner, *J. Mol. Biol.* **1993**, *233*, 629–643.

[25] B. A. Sullenger, E. Gilboa, *Nature* **2002**, *418*, 252–258.

[26] W. S. el-Deiry, T. Tokino, V. E. Velculescu, D. B. Levy, R. Parsons, J. M. Trent, D. Lin, W. E. Mercer, K. W. Kinzler, B. Vogelstein, *Cell* **1993**, *75*, 817–825.

[27] T. Miyashita, J. C. Reed, *Cell* **1995**, *80*, 293–299.

[28] S. Hasegawa, J. W. Choi, J. Rao, *J. Am. Chem. Soc.* **2004**, *126*, 7158–7159.

[29] W. Gao, B. Xing, R. Y. Tsien, J. Rao, *J. Am. Chem. Soc.* **2003**, *125*, 11146–11147.

[30] F. Michel, M. Hanna, R. Green, D. P. Bartel, J. W. Szostak, *Nature* **1989**, *342*, 391–395.

[31] G. Zlokarnik, P. A. Negulescu, T. E. Knapp, L. Mere, N. Burres, L. Feng, M. Whitney, K. Roemer, R. Y. Tsien, *Science* **1998**, *279*, 84–88.

[32] S. Hasegawa, W. C. Jackson, R. Y. Tsien, J. Rao, *Proc. Natl. Acad. Sci. USA* **2003**, *100*, 14892–14896.

[33] C. H. Contag, S. D. Spilman, P. R. Contag, M. Oshiro, B. Eames, P. Dennery, D. K. Stevenson, D. A. Benaron, *Photochem. Photobiol.* **1997**, *66*, 523–531.

[34] P. R. Contag, I. N. Olomu, D. K. Stevenson, C. H. Contag, *Nat. Med.* **1998**, *4*, 245–247.

[35] J. C. Wu, G. Sundaresan, M. Iyer, S. S. Gambhir, *Mol. Ther.* **2001**, *4*, 297–306.

[36] F. Liu, Y. Song, D. Liu, *Gene Ther.* **1999**, *6*, 1258–1266.

[37] M. Iyer, M. Berenji, N. S. Templeton, S. S. Gambhir, *Mol. Ther.* **2002**, *6*, 555–562.

[38] G. Zhang, V. Budker, J. A. Wolff, *Hum. Gene Ther.* **1999**, *10*, 1735–1737.

[39] S.-H. Hong, J.-S. Jeong, Y.-J. Lee, H.-I. Jung, K. T. Kim, Y.-H. Kim, Y.-S. Lee, S.-W. Lee, C.-D. Bae, J. Park, I.-H. Kim, *FEBS Lett.* **2007**, *581*, 5396–5400.

[40] Z. Medarova, W. Pham, C. Farrar, V. Petkova, A. Moore, *Nat. Med.* **2007**, *13*, 372–377.

[41] D. W. Bartlett, M. E. Davis, *Nucleic Acids Res.* **2006**, *34*, 322–333.

[42] A. P. McCaffrey, L. Meuse, T. T. Pham, D. S. Conkin, G. J. Hannon, M. A. Kay, *Nature* **2002**, *418*, 38–39.

[43] S. Zhao, R. D. Fernald, *J. Comput. Biol.* **2005**, *12*, 1047–1064.